International Journal of Engineering

Journal Homepage: www.ije.ir

Design and Optimization of High-gain Series and Parallel-fed Array Antennas for Enhanced Gain and Front-to-back Ratio in X-Band Applications

T. P. S. Kumar Kusumanchi*, L. Pappula

Department of Electronics and Communication Engineering, Koneru Lakshmaiah Education Foundation, AP, India

P A P E R I N F O

Paper history:
Received 26 September 2023
Received in revised form 22 November 2023
Accepted 27 November 2023

Keywords:
X-band
Antenna Array
Series Fed
Front to Back Ratio
Series Fed
Parallel Fed
Taconic

A B S T R A C T

This study presents a comprehensive analysis of the design of a high-performance meta-material loaded square patch antenna arrays specifically tailored for X-band applications. To enhance the gain and front to back ratio (FTBR), a novel 1×3 series-fed linear array configuration that integrates solitary series-fed elements with metamaterial-based square patches at X-band frequencies is introduced. Later, parallel-fed 1×2 and 1×4 antenna arrays are designed by considering the series-fed antenna array as a single element for further enhancement of gain and FTBR. The single element 1×3 series fed array is fabricated with dimensions of λ×3.5λ×0.028λ, whereas the respective 1×2 and 1×4 parallel fed antenna arrays has the dimensions of 2.86λ×3.8λ×0.028λ and 2.86λ×4.3λ×0.028λ, respectively. The Taconic substrate is chosen as the dielectric material, exhibiting a dielectric constant of 2.2 and a loss tangent of 0.0025. The empirical data presented substantiates the superior performance of the 1×4 parallel fed configuration. This is evident through the remarkable reflection coefficient of -25dB, the wide bandwidth spanning 47MHz, the substantial gain of 17.8dBi, and the FTBR of 30.7. The metrics serve to highlight the array's capacity in guaranteeing a superior level of signal fidelity, encompassing a wide frequency spectrum, amplifying incoming signals, and directing transmissions towards specific orientations. These metrics unequivocally validate its potential for advanced X-band applications.

***doi**: 10.5829/ije.2024.37.03c.12*

Graphical Abstract

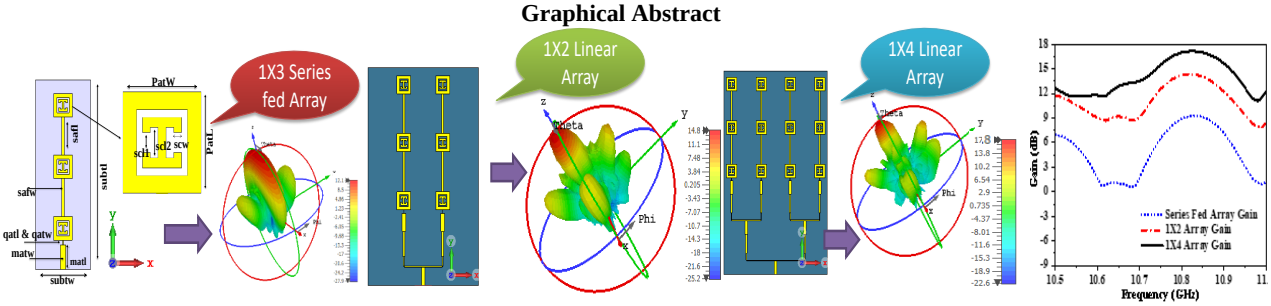

1. INTRODUCTION

The X-band, encompassing frequencies spanning from 8.0 GHz to 12.0 GHz, assumes a pivotal role within the electromagnetic spectrum, occupying a distinct position that facilitates its utilization across diverse domains such as radar systems, satellite communications, remote sensing, and scientific inquiry. In order to optimize the utilization of X-band technology, it is crucial to prioritize the advancement of antenna systems. The primary instantiation of remote sensing entails the application of satellite communication systems, contingent upon the condition of an atmosphere devoid of cloud cover, to acquire data of utmost quality. The effectiveness of

*Corresponding Author Email: satishkumar8421@gmail.com (T. P. S. Kumar Kusumanchi)

Please cite this article as: Kumar Kusumanchi TPS., Pappula L. Design and Optimization of High-gain Series and Parallel-fed Array Antennas for Enhanced Gain and Front-to-back Ratio in X-Band Applications. International Journal of Engineering, Transactions C: Aspects. 2024;37(03):546-55.

satellite communication systems has been observed to be constrained during periods of reduced illumination, unfavorable meteorological circumstances such as storms, and in areas distinguished by high levels of vegetation coverage.

The central constituent of the x-band communication system is the sensing module, more precisely denoted as the Antenna module. In contemporary times, the escalating occurrence of perilous meteorological phenomena on a worldwide scale has instigated a notable upsurge in scholarly attention towards the investigation of economically viable and compact synthetic aperture radar (SAR) systems deployed in space (1). These technological systems exhibit significant promise in the realm of monitoring and evaluating natural disasters, encompassing a wide range of events such as tsunamis, typhoons, landslides, and volcanic eruptions. Their efficacy is particularly noteworthy in nations that are susceptible to these catastrophic occurrences (2). The antenna demonstrates multi-band functionality, accommodating both horizontal and vertical polarizations, thus serving as a vital constituent in synthetic aperture radar (SAR) systems. Both co-polarization and cross-polarization are essential elements in enabling the Synthetic Aperture Radar (SAR) antenna to efficiently capture and acquire data with exceptional detail (3). There is an imperative to alleviate the complexity associated with SAR antenna design, while also minimizing its physical dimensions, mass, and costs. This must be achieved while ensuring that the antenna meets the specified requirements for enhanced gain, multiple frequency bands, and dual polarizations. Owing to the exorbitant financial expenditure, considerable mass, and cumbersome physical proportions of the antennas utilized in synthetic aperture radar (SAR) applications. The X-band synthetic aperture radar (SAR) demonstrates a notable level of appropriateness for reconnaissance and disaster monitoring purposes, primarily due to its remarkable spatial resolution capabilities. Therefore, it is considered the most suitable option for the purpose of surveillance (4).

The effectiveness of systems undergoes degradation as a result of multiple factors, specifically side-lobe level, cross-polarization, co-polarization, front-to-back ratio, and half power beam width (HPBW) (5). In this particular instance, the radar antenna proficiently acquired the echo signal through the utilization of the back lobe or side lobe, facilitated by the presence of numerous reflections. Likewise, the transmission signals experienced scattering in a similar manner. This phenomenon leads to the detection of inaccuracies within the designated data, consequently leading to the manifestation of erroneous alerts. Microstrip antenna arrays, colloquially referred to as MSA arrays, manifest substantial promise across diverse domains, encompassing radar systems, satellite communications, and wireless communication networks. The reduced mass, cost-effectiveness, and seamless compatibility with the feed network are key attributes of the aforementioned (6, 7). Arraying is a widely utilized technique in long-distance communication networks for the purpose of amplification enhancement. Arrays can be categorized into two discrete classifications based on their feeding methodology, specifically parallel-fed arrays and series-fed arrays (8).

The design of the feed network plays a pivotal role in configuring arrays of microstrip antennas (MSAs). In the context of microstrip arrays, employing a series feed mechanism that seamlessly integrates with each radiating element facilitates achieving in-phase excitation while ensuring consistent amplitude across these elements. However, this approach leads to increased side lobe levels (SLL) and heightened losses in the feedlines. The utilization of a technique referred to as series-feed has been implemented to address the issue of signal leakage and reduce losses in the feedline. This methodology presents the benefit of occupying a diminished physical space while efficiently tackling the aforementioned concerns. Furthermore, it is pertinent to highlight that array antenna configurations employing printed circuit boards (PCBs) exhibit distinctive attributes, including a reduced physical footprint and a lightweight construction. The aforementioned attributes render them exceptionally well-suited for implementation in millimeter-wave (MMW) scenarios, outperforming preceding metal-based configurations such as four quadrant horn arrays with reflectors and waveguide slot arrays (9, 10). Numerous comprehensive research studies have explored microstrip arrays, employing both parallel and series feed techniques (11-16), plate slot arrays (17), and substrate integrated waveguide (SIW) slot arrays (18-22).

Significant attention has been directed towards microstrip arrays, primarily due to their relatively simplified manufacturing process in comparison to substrate integrated waveguide (SIW) structures. Furthermore, these arrays offer improved convenience in achieving desired radiation patterns through various configurations of constituent elements and feed networks (23). The investigation employed a configuration comprising of six series-fed microstrip linear subarrays, as elucidated in the reference (24). The implemented configuration featured a distribution of tapered patch widths. The integration of the subarrays was accomplished by employing a single-end connecting Substrate Integrated Waveguide (SIW) parallel feed network. The configuration was intricately designed to manipulate geometric formations in both the horizontal and vertical cross-sectional planes. The investigation carried out by Zhao et al. (25) employed a set of patches featuring gradually decreasing widths and impedance transformers to construct a planar microstrip array that

was specifically engineered for the task of long-range automobile radar detection. Remarkably, an admirable accomplishment was observed in achieving an optimal first side lobe level (FSLL) of approximately -20 dB in both the E and H planes. Furthermore, the previously mentioned by Kothapudi and Kumar (26, 27) elucidated the execution of a 6-port 3 × 3 series-fed planar array and a 4-port 2 × 2 series-fed planar array, correspondingly. Both of these designs integrated excitations originating from two orthogonal directions, employing a chosen configuration to confer dual-polarized characteristics upon the arrays. The aforementioned attribute rendered them exceedingly suitable for integration into X-band airborne synthetic aperture radar (SAR) systems. Moreover, a K-band linear array comprising ten series-fed rectangular patches was postulated by Bayderkhani and Hassani (28).

This paper introduces a novel approach by incorporating series feeding, along with the utilization of a parallel feeding in the design. The results demonstrate the ability to accommodate a greater number of radiating elements in confined space, leading to the achievement of high gain. In contrast to conventional designs employing normal square patches, this study utilizes metamaterial square patches. The use of metamaterials allows for the creation of antenna elements with unique electromagnetic properties, facilitating miniaturization and enabling features such as Frequency Selectivity, Steerable, and Reconfigurable Antennas. The primary objective of this research is to design and fabricate a compact series-fed linear array tailored for X-band applications. The developed antenna prototype ensures optimal functionality at a frequency of 10.76GHz, placing it within the X-band spectrum.

This investigation employed Taconic TLY-5 as the substrate material due to its capacity to offer a diverse range of impedance bandwidth, peak gain, and high radiation efficiency. The final iteration of the antenna prototype features physical dimensions of 80×50×0.8mm³, operating at a frequency of 10.76 GHz. To optimize gain and FTBR (Front-to-Back Ratio), linear array configurations, specifically a 1×2 and a 1×4 parallel fed linear array, were implemented. These arrays exhibit minimal mutual coupling among their constituent elements, resulting in enhanced overall performance. The system demonstrated a notable improvement in amplification, making it well-suited for applications in the X-band.

The main objective of the paper is to present the design of a high gain and FTBR series-fed antenna arrays at X band frequencies. To realize, we introduced a novel unique 1×3 series-fed linear array configuration that integrates solitary series-fed elements with metamaterial-based square patches. Later, parallel-fed 1×2 and 1×4 antenna arrays are designed by considering the series-fed antenna array as a single element for further enhancement of gain and FTBR.

The geometry of the proposed 1×3 series-fed antenna array with metamaterial-loaded rectangular patches is discussed in section 2. The selection mechanism of the proposed antenna array parameters is discussed in section 3. Section 4 presents elaborate discussions on the measured results of the proposed antenna array. In section 5, the design of parallel-fed 1×2 and 1×4 antenna arrays for further enhancement of gain and FTBR is discussed by considering the series-fed antenna array as a single element. The complete discussion of the proposed arrays' radiation characteristics is discussed in section 6. Section 7 summarizes the final conclusions of the article.

2. DESIGN OF BASIC 1×3 SERIES-FED ANTENNA ARRAY

Microstrip patch antennas are fabricated utilizing a dielectric substrate, which is encased by a conductive layer on both sides. In contrast, the upper surface of the substrate is incompletely covered, serving as the exclusive location for the patch elements and feeding line. The substrate material utilized in this investigation is Taconic TLY5, which possesses a dielectric constant of 2.2 and a loss tangent of 0.002. The substrate possesses a vertical dimension of 31 mil and is furnished with a copper cladding of 1 oz on each of its surfaces.

Antenna arrays combine multiple radiating elements, and feeding methods are critical in their architecture. Series feeding connects the primary feed line to all elements, while series feeding links components sequentially. In linear fed arrays, the primary element emits radiation, cascading feed power to subsequent elements.

The basic antenna configuration comprises a metamaterial loaded square patches are connected in series with a 50-Ω microstrip line, with a quarter-wave transformer etched onto the substrate's top surface. The matching between the radiating square patch and the 50-Ω microstrip line is achieved through a quarter-wave transformer. The current research endeavors to examine the stimulation of this sequence of elements by employing a unique feed port that has been meticulously designed to function at a precise frequency of 10.73 gigahertz. The array is stimulated directly via a microstrip feed line, wherein the series feeding of the array elements is situated at the uppermost region of the substrate. The terrestrial surface, conversely, is situated in the lowermost stratum of the substrate.

The Square patch width ‘W’ and length ‘L’ are calculated from the following expressions 1& 2.

$$W = \frac{(2M+1)}{\sqrt{\frac{\varepsilon_r+1}{2}}} \times \frac{\lambda_0}{2} \quad (1)$$

$$L = \frac{(2N+1)}{\sqrt{\varepsilon_{eff}}} \times \left(\frac{\lambda}{2}\right) - 2 \times \Delta L \quad (2)$$

where M and N are non-negative integers (in our present design M=N=1).

The feedline width calculated by using below Equation 3.

$$W = \frac{7.48 \times h}{e^{\left(z_0 \frac{\sqrt{\varepsilon_r}+1.41}{87}\right)}} - 1.25 \times t \quad (3)$$

where h is height of the substrate t is the thickness of the copper.

The diagram depicted in Figure 1 showcases the geometric arrangement of a 1×3 series-fed square patch linear array, which includes a single RF antenna port. The process of optimizing a finite set of parameters at the resonant frequency of 10.76 gigahertz results in the attainment of the most advantageous reflection coefficient. The series-fed square patch linear array, possessing dimensions of 1×3, was efficiently fed by employing a matching transformer and a λ/4 impedance transformer. Both the matched transformer and the λ/4 impedance transformer are employed to optimize impedance matching between the radiating array and the feed. The establishment of a direct or series connection between the square elements is accomplished by utilizing microstrip lines with precise dimensions of safl and safw. The impedance characteristics of the matched transformer, quarter-wavelength impedance transformer, and matched feedlines interconnecting the patches are dependent on the dimensional attributes of the corresponding feedlines. The dimensional parameters of the matched transformer and λ/4 impedance transformer are denoted as matl, matw, qatl, and qatw, correspondingly.

Optimization techniques are utilized in order to augment the operational efficacy of the array, thereby facilitating the attainment of utmost gain and enhanced impedance matching. The present array is comprised of a solitary RF antenna port exhibiting a return loss characteristic. The array under consideration

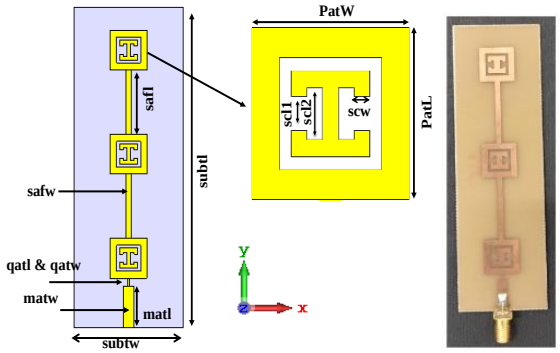

Figure 1. Construction and fabricated model of the basic 1×3 series fed antenna array

demonstrates an impedance bandwidth spanning from 10.70 GHz to 10.74 GHz, with a bandwidth of 40 MHz.

Figure 2 depicts the surface current distribution, as well as the impact of the electric field (E-field) and magnetic field (H-field), for a 1×3 series-fed square patch linear array. This array is equipped with a single radio frequency (RF) antenna port, and the simulation was conducted using CST simulation software. The simulation was carried out with carefully optimized parameters. The specified dimensions for the optimized construction of the proposed 1×3 series -fed square patch linear array antenna are presented in Table 1.

3. SELECTION OF OPTIMAL PARAMETERS

The goal of the study was to determine the best parameters for a single RF antenna to analyze the

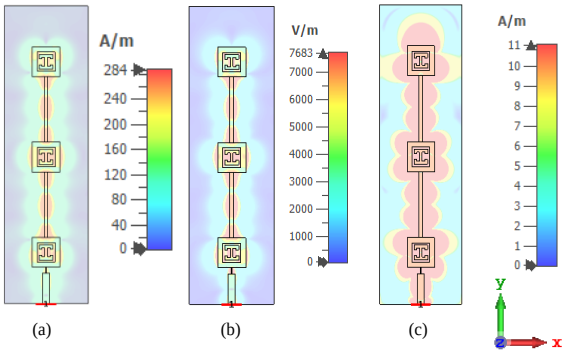

Figure 2. a) surface current, b) magnitude of E-field c) magnitude if H-field of the basic 1×3 series fed antenna array

TABLE 1. Geometrical Parameters of Antenna Array

Parameter	Parameter Description	Value (mm)
PatL	Square patch Length	10
PatW	Square patch Width	10
qatl	λ/4 impedance transformer Length	2
qatw	λ/4 impedance transformer Length Width	0.28
matl	Impedance Matching Transformer Length	10.25
matw	Impedance Matching Transformer Width	2.46
safl	Length of the series-fed line	22
safw	Width of the series-fed line	1.9
subtl	Antenna Substrate Length	80
subtw	Antenna Substrate Width	50
subth	Antenna Substrate Heigth	0.787
scw	Slot width	1
sc11	Slot1 small length	2
scl2	Slot1 long length	3

reflection coefficient of a proposed 1×3 series-fed square patch linear array. The matched transformer, λ/4 impedance transformer, and serried feedline dimensions are optimized, and the effect of their variation on return loss is investigated. The parameters that have been optimized include matw, matl, qatw, qatl, safw, and safl. The process of optimization entailed optimizing each parameter one at a time, holding the other parameters constant. Best results and improved impedance matching were found at qatl=2.8mm, qatw=0.5, matl=12mm, matw=3mm, safl=11mm, and safw=1.5mm using simulation software. Figure 3(a-e) presents a visual representation of the optimization results related to the suggested antenna.

3. 1. Varying Qatl Figure 3a depicts the impact of varying the length of the λ/4 impedance transformer, with precise adjustments made in 0.2mm increments within the range of 1.5 to 5mm. Other parameters (qatw, matw, matl, safw, and safl) remain constant throughout the experiment. Superior impedance matching was achieved at 2.8 millimeters, resulting in favorable resonance at a frequency of 10.736GHz. The simulation indicated the antenna's operation within the X-band frequency range, specifically between 10.70GHz and 10.74GHz.

3. 2. Varying qatw In Figure 3b, the impact of varying the width of the λ/4 impedance transformer is illustrated, with precise adjustments made using a 0.03mm step size within a range of 0.3mm to 1.5mm. Remaining parameters (qatl, matw, matl, safw, and safl) were held constant. Optimal impedance matching was achieved at a width of 0.5 millimeters. Simulation results showed resonance at 10.736 GHz, indicating excellent impedance matching, and the antenna functioned within the 10.70GHz to 10.74GHz X-band frequency range.

3. 3. Varying matl Figure 3c illustrates the impact of varying the length of the matched transformer, systematically adjusted within the range of 5mm to 15mm with a 0.1mm step size. Parameters qatw, matw, qatl, safw, and safl are held constant. Enhanced impedance matching was observed at a length of 12 millimeters. Simulation results revealed resonance at 10.736GHz, indicating commendable impedance matching, and the antenna operated within the X-band frequency range, specifically between 10.70GHz and 10.74GHz.

3. 4. Varying matw Figure 3d demonstrates the impact of varying the width of the matched transformer, systematically adjusted within the range of 2 to 4mm with a 0.1mm step size. Parameters qatw, mqatl, matl, safw, and safl are held constant. Superior impedance matching was achieved at a width of 3 millimeters. Simulation results indicated resonance at 10.736 GHz, showcasing commendable impedance matching, and the antenna operated within the X-band frequency range, specifically between 10.70GHz and 10.74GHz.

3. 5. Varying Safw In Figure 3e, the impact of varying the width of the series feedline connecting the patches is depicted, systematically adjusted within the range of 0.5mm to 3.5mm with a 0.2mm step size. Parameters qatw, matw, matl, qatl, and safl are held constant. Enhanced impedance matching was observed at a width of 1.5 millimeters. Simulation results indicated resonance at 10.736GHz, demonstrating commendable impedance matching, and the antenna operated within the X-band frequency range, specifically between 10.70GHz and 10.74GHz.

4 TEST RESULTS OF BASIC 1×3 SERIES FED ANTENNA ARRAY

The 1×3 series-fed square patch linear array, designed for X-band operation, has been fabricated and measured to validate simulation results. Figure 1 illustrates the fabricated prototype. Both simulated and measured data juxtaposition at the operational frequency range within the X-band. Figure 4a presents a comparison of simulated and fabricated reflection coefficients and it's demonstrates an impedance bandwidth of 40MHz, ranging from 10.70 GHz to 10.74 GHz, with a gain of 12.8dB. The electrical field the series fed array oriented perpendicular to the surface of the radiating patch, defining it as a vertically polarized antenna array. This

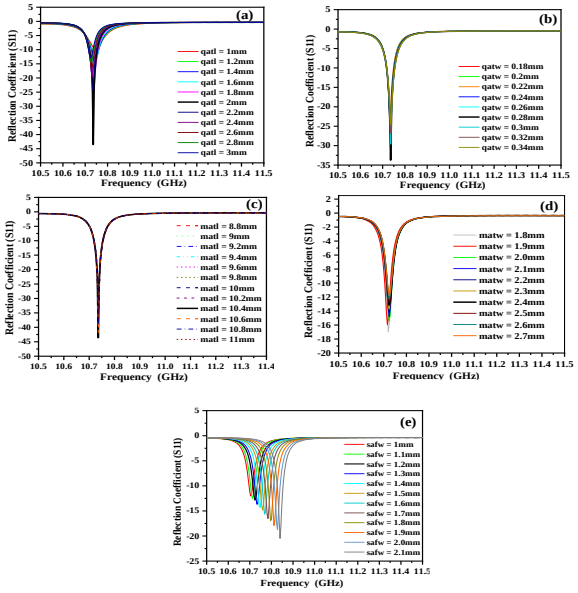

Figure 3. Reflection Coefficient of proposed antenna with various parameters a) qatl, b) qatw, c) matl, d) matw & e) safw

characteristic underscores the array's alignment for effective vertical polarization in its radiation pattern.

Figure 4(b & c). represents 2D Co and cross polarization graph of the proposed series fed element at 10.73 GHz. The outcome indicates that the radiation patterns exhibit directive characteristics, are vertically polarized, and have minimal sidelobe levels.

5. DESIGN OF PARALLEL FED 1×2, ANF 1×4 ANTENNA ARRAY IMPLEMENTATION

High gain antennas are essential for efficient signal propagation over long distances. Increasing antenna gain often involves using an array of elements rather than a single one. The cardinality of the array, or the number of elements, directly correlates with the antenna's gain. The signal feed network, distributing power across branches, is crucial in high-gain antenna construction. Variations in power divider arm length and width impact signal amplitude and phase, leading to changes in the angular range of beam scanning.

The array configuration employs parallel feeding with microstrip transmission lines for power division between the primary port and radiating elements. Linear power dividers (LPDs) are fabricated using a simple arrangement, dividing a single microstrip transmission line into two to bifurcate power into separate paths. The 1×4 parallel fed power divider arrangements, as depicted in Figure 5.

The selection was made to utilize the parallel or corporate feed methodology for the purpose of dividing the power into two distinct transmission lines. The proposed configuration involves the fabrication of a 1 x 2 array structure, accomplished by spatially segregating two 1×3 series-fed square patch linear arrays. The intentional setting of the separation distance between the individual elements is half of the wavelength.

The rationale behind this design decision is to effectively address the issue of gating lobes, which have the potential to negatively affect the overall performance of the array. The integration of a Stranded T-Junction power divider has been successfully incorporated into the corporate feed network design for the 1×2 parallel fed array. The Maximum Power Transfer Theorem is a fundamental principle widely utilized in the field of electrical engineering to facilitate the attainment of impedance matching. To augment the antenna gain, a configuration is deployed whereby two 1×2 corporate feeding networks are interconnected consecutively, leading to the establishment of a 1×4 parallel fed array. Through the utilization of a quarter-wave transformer, the transmission lines possessing an impedance of 100Ω are efficiently transformed into transmission lines exhibiting an impedance of 70.7Ω. Following this, the aforementioned lines are subsequently aligned with an inset feed configuration possessing an impedance of 50 Ω. The diagram illustrated in Figure 6 represents a unidimensional array with a size of 1×2. In contrast, the structure depicted in Figure 7 exemplifies a

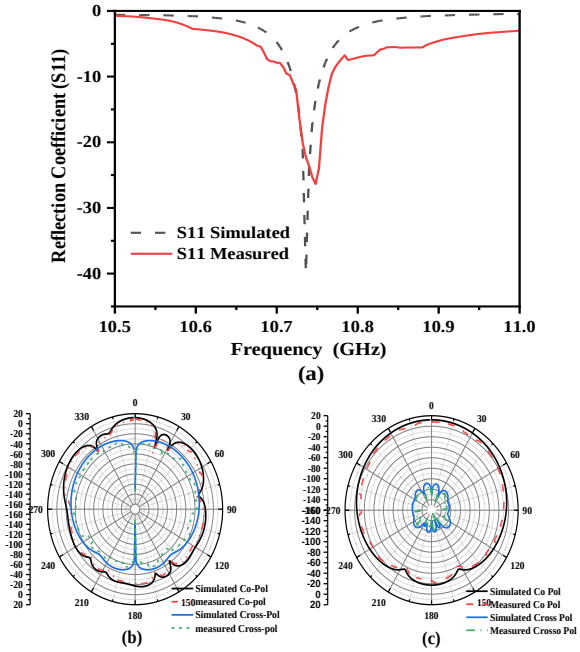

Figure 4. (a)Reflection Coefficient of proposed antenna (b) Gain theta Co and Cross polarization, (c) Gain Phi Co and Cross polarization

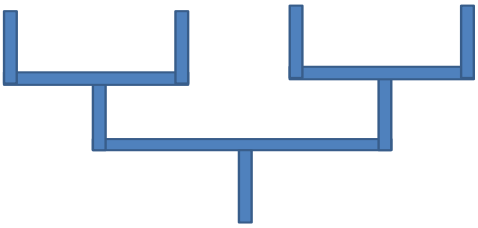

Figure 5. 1×4 parallel fed Power Divider

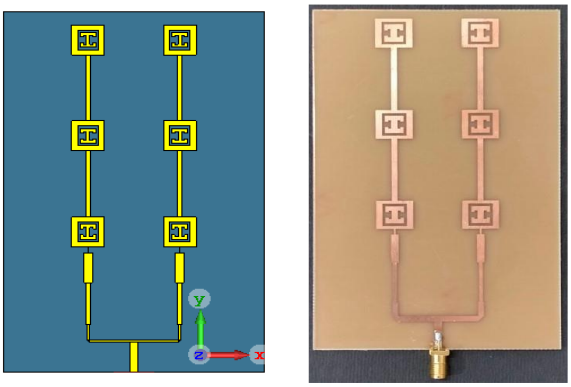

Figure 6. Simulated and fabricated model of 1×2 parallel fed antenna array

unidimensional array characterized by dimensions of 1×4 parallel fed antenna array.

6. RESULTS AND DISCUSSION

6. 1. Return Loss Figures 8a and 8b depict the S11 parameters, which represent the reflection coefficient of the 1×2 and 1×4 parallel fed antenna arrays. The single-element patch antenna resonates at 10.732 GHz with a reflection coefficient of -34 dB and a bandwidth of 40 MHz. In the 1×2 parallel fed antenna array configuration, the antenna shows a return loss of -26.99 dB and a bandwidth of 37 MHz, peaking at a resonant frequency of 10.74 GHz. The 1×4 array antenna displays a reflection coefficient of -25.76 dB and a broader bandwidth of 47 MHz.

6. 2. Directivity The directivity of a single element, 1×2, and 1×4 parallel fed antenna array at a frequency of 10.74 GHz was measured to determine the level of radiation intensity. The measured directivity was found to be 17.8dBi, which quantifies the amount of radiation emitted by the antenna. The directivity values for the single element, 1×2, and 1×4 parallel fed antenna array configurations are recorded as 13.52 dBi, 16.50 dBi, and 17.9 dBi, respectively. The directivity of a 1 x 4 array of serried fed linear array exhibits superior performance in comparison to that of a single element antenna and a 1 x 2 array antenna.

6. 3. Gain Figure 9 illustrates the Gain plot of a single element, 1 x 2, and 1 x 4 array antenna operating at a frequency of 10.74 GHz. The Gain plot exhibits a gain value of 17.8 dBi. The 1×3 series fed single element, 1×2, and 1×4 parallel fed antenna array configurations have achieved gains of 12.1 dBi, 14.9 dBi, and 17.8 dBi, respectively. The performance of a 1×4 parallel fed linear array exhibits superior gain when compared to that of a 1×3 series fed single element antenna and a 1×2 parallel fed antenna antenna.

6. 4. Co and Cross Polarization Figure 10 (a & b) depicts the two-dimensional co-polarization and cross-polarization characteristics of the 1×2 parallel fed antenna array operating at a frequency of 10.74 GHz and Figures 11a, and 11b represents the two-dimensional co-polarization and cross-polarization characteristics of the array antennas operating at a frequency of 10.74 GHz. Based on the obtained results, it can be observed that the radiation patterns exhibit a directive characteristic. The current antenna arrays' Co and cross polarization graphs indicate that they possess cross polarization levels within acceptable limits and exhibit minimal side lobe levels (SLL). Figures 12a,12b, and 12c are represent the 3-dimensional gain of the 3 proposed arrays.

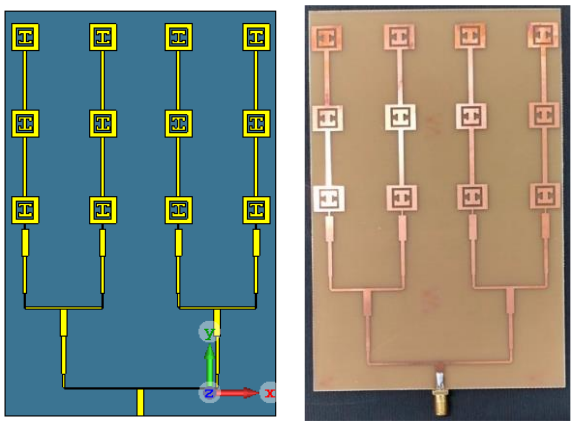

Figure 7. Simulated and fabricated model of 1×4 parallel fed antenna array

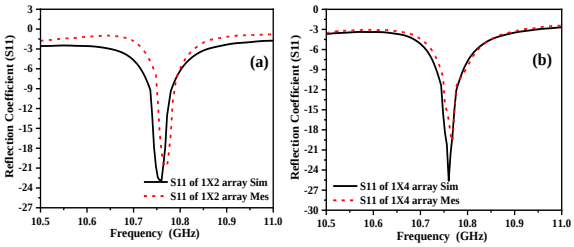

Figure 8. a & b Simulated and Fabricated Reflection coefficient of 1×2 and 1×4 parallel fed antenna array

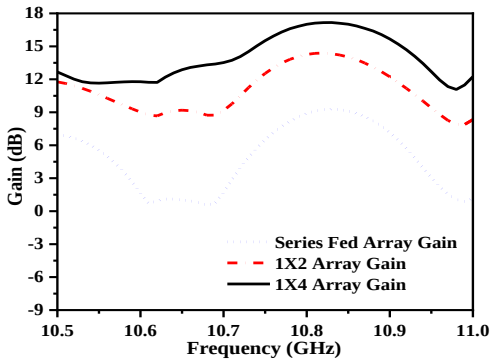

Figure 9. Gain Comparison between the Proposed 1×3 series fed, 1×2 and 1×4 parallel fed antenna arrays

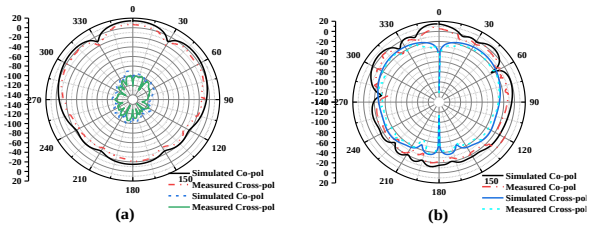

Figure 10. a & b 1×2 parallel fed array gain phi & theta co and cross polarization

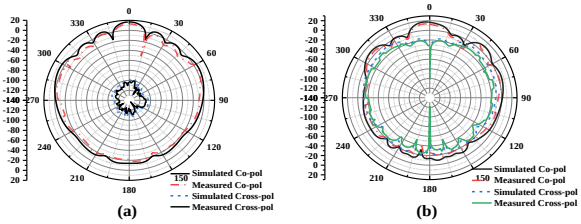

Figure 11. a & b 1×4 parallel fed array gain phi & theta co and cross polarization

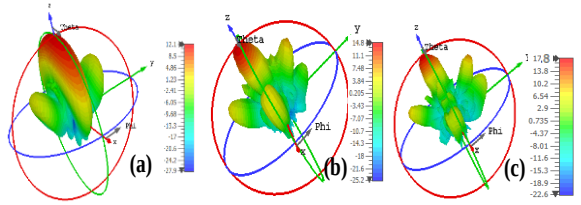

Figure 12. 3-Dimentional gain a)1×3 series fed b) 1×2 parallel fed, & c) 1×4 parallel fed antenna array

The performance characteristics of a single 1×3 series-fed, 1×2 parallel fed, and 1×4 parallel fed Microstrip patch antenna array are presented in Table 2.

Table 3 provides a thorough comparison of crucial parameters, encompassing antenna size, antenna gain, sidelobe levels, efficiency and FTBR, across the various designs proposed. This in-depth analysis aims to underscore the merits of the proposed antenna array designs, spanning from the 1×3 series-fed array to the 1×4 parallel fed linear array. The comparison specifically emphasizes the advantages such as substantial gain improvement, favorable FTBR.

A high FTBR in this context signifies that the proposed array exhibits maximum gain radiation in a specific direction, accompanied by low sidelobes. It serves as a key indicator of the array's effectiveness in focusing its radiation in the desired direction. However, it's essential to acknowledge a limitation of the proposed array, which lies in its suitability primarily for narrow-band applications.

TABLE 2. Comparison between the 3 proposed antenna arrays

Parameter		1×3 Series Fed antenna array	1×2 parallel fed antenna array	1×4 array parallel fed antenna array
Bandwidth		10.719-10.754 GHz (35MHz)	10.74-10.77 GHz (37MHz)	10.739-10.78 6GHz (47MHz)
Resonant Frequency		10.736GHz	10.76GHz	10.76GHz
Gain		12.1dB	14.8dB	17.8dB
Radiation Efficiency		82%	84%	86%
E-plane	SLL(dB)	-10.6dB	-9.5	-11.4
	HPBW(deg)	16.5	15.2	12.6
	Cross Pol(dB)	-24.2	-13.2	-10.7
	FTBR	30	25.6	30.7
H-plane	SLL(dB)	-10.6dB	-9.5	-11.4
	HPBW(deg)	16.5	15.2	12.6
	Cross Pol(dB)	-92	-90.2	-96.7
	FTBR	30	28.6	30.7

TABLE 3. Comparison of proposed work with previous series fed arrays

Ref no	No.of patches	Size (mm)	Working band	Gain	SLL	FTBR
(11)	2×2 patch array	50x42	X	12.4	-19	30
(12)	21×4 patch array	240 dia	X	22.4	-15	NA
(13)	4×4 patch array	210x210	C	18.4	-12	NA
(16)	Radial wave guide slot array	80 dia	X	18.1	-14.9	NA
(22)	3×3	80x80	K	12.2	-25.4	31
(23)	1×10	100x15	K	17.4	-26.3	37
(24)	6×6	150x150	X/K	17.2	-15	37
(8)	2×2	77x24	C	13.95	NA	NA
(11)	2×2	84x45	X	13.4	-19	NA
This work	**Series fed(1×3)**	**80x50**	**X**	**12.1**	**-10.6**	**۳۰**
This work	**1×2 parallel fed antenna array**	**120x100**	**X**	**14.8**	**-11.5**	**28.6**
This work	**1×4 parallel fed antenna array**	**150x120**	**X**	**17.4**	**-15**	**30.7**

7. CONCLUSION

A unique 1×3 series-fed linear array setup that integrates individual series-fed elements with square patches based on metamaterials at X-band frequencies is developed and discussed in this article. Furthermore, parallel-fed 1×2 and 1×4 antenna arrays are designed by considering the series-fed antenna array as a single element is designed. The outcomes of this design process encompass essential parameters such as the reflection coefficient, bandwidth, directivity, gain, and front-to-back ratio for all three proposed designs. The gain and FTBR are significantly increased while operating at the desired frequencies around 10.76 GHz. For example, it has been determined that the parallel fed 1×4 linear array is resonated with a bandwidth of 47 MHz at 10.76 Ghz. The measured gain is 17.8dBi, signifies the array's capacity to augment the received signal by amplifying its strength and enhancing its overall quality. It produced FTBR of 30.7 and radiation efficiency of 86%. All the designed arrays are vertically polarized. These obtained metrics offer a superior level of signal fidelity, amplify incoming signals, and direct transmissions towards specific orientations. The potential of the proposed arrays for advanced X-band applications is unequivocally confirmed by these metrics.

8. REFERENCES

1. Ravindra V, Akbar PR, Zhang M, Hirokawa J, Saito H, Oyama A. A Dual-Polarization $ X $-Band Traveling-Wave Antenna Panel for Small-Satellite Synthetic Aperture Radar. IEEE Transactions on Antennas and Propagation. 2017;65(5):2144-56. 10.1109/TAP.2017.2676760
2. Mao C-X, Gao S, Tienda C, Rommel T, Patyuchenko A, Younis M, et al. X/Ka-band dual-polarized digital beamforming synthetic aperture radar. IEEE Transactions on Microwave Theory and Techniques. 2017;65(11):4400-7. 10.1109/TMTT.2017.2690435
3. Rabideau DJ, Parker P, editors. Ubiquitous MIMO multifunction digital array radar. The Thrity-Seventh Asilomar Conference on Signals, Systems & Computers, 2003; 2003: IEEE.
4. Kuo F-Y, Hwang R-B. High-isolation X-band marine radar antenna design. IEEE Transactions on Antennas and Propagation. 2014;62(5):2331-7. 10.1109/TAP.2014.2307296
5. Skolnik MI. Radar handbook. 1970.
6. Li M, Tian S, Tang M-C, Zhu L. A compact low-profile hybrid-mode patch antenna with intrinsically combined self-decoupling and filtering properties. IEEE Transactions on Antennas and Propagation. 2021;70(2):1511-6. 10.1109/TAP.2021.3111638
7. Chang L, Liu H. Low-profile and miniaturized dual-band microstrip patch antenna for 5G mobile terminals. IEEE Transactions on Antennas and Propagation. 2021;70(3):2328-33. 10.1109/TAP. 2021.3118730
8. Wang B, Zhao Z, Sun K, Du C, Yang X, Yang D. Wideband Series-Fed Microstrip Patch Antenna Array With Flat Gain Based on Magnetic Current Feeding Technology. IEEE Antennas and Wireless Propagation Letters. 2022;22(4):834-8. 10.1109/LAWP.2022.3226461
9. Ling C, Rebeiz GM. 94 GHz integrated horn monopulse antennas. IEEE transactions on antennas and propagation. 1992;40(8):981-4. 10.1109/8.163437
10. Soltan A, Neshati M. Design and Development of High Gain, Low Profile and Circularly Polarized Cavity-backed Slot Antennas Using High-order Modes of Square Shaped Substrtae Integrated Waveguide Resonator. International Journal of Engineering, Transactions C: Aspects. 2017;30(12):1840-7. 10.5829/ije.2017.30.12c.04
11. Khatami SA, Meiguni J, Elahi AA-e, Rezaei P. Compact via-coupling fed monopulse antenna with orthogonal tracking capability in radiation pattern. IEEE Antennas and Wireless Propagation Letters. 2020;19(8):1443-6. 10.1109/LAWP.2020.3005023
12. Kumar H, Kumar G. Broadband monopulse microstrip antenna array for X-band monopulse tracking. IET Microwaves, Antennas & Propagation. 2018;12(13):2109-14. 10.1049/iet-map.2018.5332
13. Lamultree S, Phalla M, Kunkritthanachai P, Phongcharoenpanich C. Design of a Circular Patch Antenna with Parasitic Elements for 5G Applications. International Journal of Engineering. 2023;36(9):1686-94. 10.5829/ije.2023.36.09c.13
14. Fakharian M. A wideband fractal planar monopole antenna with a thin slot on radiating stub for radio frequency energy harvesting applications. International Journal of Engineering, Transactions B: Applications 2020;33(11):2181-7. 10.5829/IJE.2020.33.11B.08
15. Atamanesh M, Abbasi Arand B, Zahedi A. Wideband microstrip antenna array with simultaneously low sidelobe level in both sum and difference patterns. IET Microwaves, Antennas & Propagation. 2018;12(5):820-5. 10.1049/iet-map.2017.0494
16. Contreras A. Objective Functions for the Optimization of an Ultra Wideband Antenna. International Journal of Engineering. 2021;34(7):1743-9. 10.5829/ije.2021.34.07a.19
17. Aliasgari J, Atlasbaf Z. A novel compact monopulse parallel-plate slot array antenna. IEEE Antennas and Wireless Propagation Letters. 2015;15:762-5. 10.1109/LAWP.2015.2472462
18. Ying F, Ahmed F, Li R. A multiband multiple-input multiple-output antenna system for long term evolution and wireless local area networks handsets. International Journal of Engineering, Transactions B: Applications 2016;29(8):1087-93. 10.5829/idosi.ije.2016.29.08b.08
19. Cheng YJ, Hong W, Wu K. 94 GHz substrate integrated monopulse antenna array. IEEE transactions on antennas and propagation. 2011;60(1):121-9. 10.1109/TAP.2011.2167945
20. Dashti H. Design investigation of microstrip patch and half-mode substrate integrated waveguide cavity hybrid antenna arrays. International Journal of Engineering, Transactions B: Applications 2015;28(5):686-92. 10.5829/idosi.ije.2015.28.05b.06
21. Li W, Liu S, Deng J, Hu Z, Zhou Z. A compact SIW monopulse antenna array based on microstrip feed. IEEE Antennas and Wireless Propagation Letters. 2020;20(1):93-7. 10.1109/LAWP.2020.3041485
22. Yang T, Zhao Z, Yang D, Liu X, Liu Q-H. A single-layer SIW slots array monopulse antenna excited by a dual-mode resonator. IEEE Access. 2019;7:131282-8. 10.1109/ACCESS.2019.2940635
23. Menzel W, Moebius A. Antenna concepts for millimeter-wave automotive radar sensors. Proceedings of the IEEE. 2012;100(7):2372-9. 10.1109/JPROC.2012.2184729
24. Xu J, Hong W, Zhang H, Wang G, Yu Y, Jiang ZH. An array antenna for both long-and medium-range 77 GHz automotive radar applications. IEEE transactions on antennas and propagation. 2017;65(12):7207-16. 10.1109/TAP.2017.2761549

25. Zhao J, Zou L, Jiang R, Wang X, Gao H. Hybrid antenna arrays with high angular resolution for 77 GHz automotive radars. IEICE Electronics Express. 2020;17(2):20190687-. 10.1109/TAP.2017.2761549

26. Kothapudi VK, Kumar V. A 6-Port Two-Dimensional 3×3 Series-Fed Planar Array Antenna for Dual-Polarized X-Band Airborne Synthetic Aperture Radar Applications. Ieee Access. 2018;6:12001-7. 10.1109/ACCESS.2018.2810233

27. Kothapudi VK, Kumar V. Compact 1× 2 and 2× 2 dual polarized series-fed antenna array for X-band airborne synthetic aperture radar applications. Journal of electromagnetic engineering and science. 2018;18(2):117-28. 10.26866/jees.2018.18.2.117

28. Bayderkhani R, Hassani HR. Wideband and low sidelobe slot antenna fed by series-fed printed array. IEEE Transactions on Antennas and Propagation. 2010;58(12):3898-904. 10.1109/TAP.2010.2078437

Persian Abstract

چکیده

این مطالعه یک تجزیه و تحلیل جامع از طراحی آرایه‌های آنتن مربعی بارگذاری شده با متا مواد با کارایی بالا ارائه می‌کند که به طور خاص برای کاربردهای باند X طراحی شده است. برای افزایش بهره و نسبت جلو به عقب (FTBR)، یک پیکربندی جدید آرایه خطی با تغذیه سری ۱×۳ که عناصر تغذیه‌شده سری منفرد را با تکه‌های مربعی مبتنی بر فراماده در فرکانس‌های باند X معرفی می‌کند. بعدها، آرایه های آنتن ۱×۲ و ۱×٤ با تغذیه موازی با در نظر گرفتن آرایه آنتن سری به عنوان یک عنصر واحد برای افزایش بیشتر بهره و FTBR طراحی می شوند. آرایه تغذیه سری ۱×۳ تک عنصری با ابعاد $\lambda\times3.5\lambda\times0.028\lambda$ ساخته شده است، در حالی که آرایه های آنتن تغذیه موازی ۱×۲ و ۱×٤ دارای ابعاد $\lambda\times4.3\lambda\times0.028\lambda$ و $\lambda\times3.8\lambda\times0.028\lambda$ ۲.۸٦ است. به ترتیب. بستر Taconic به عنوان ماده دی الکتریک انتخاب می شود که ثابت دی الکتریک ۲.۲ و مماس تلفات ۰.۰۰۲۵ را نشان می دهد. داده های تجربی ارائه شده، عملکرد برتر پیکربندی تغذیه موازی ۱×٤ را اثبات می کند. این امر از طریق ضریب بازتاب قابل توجه ۲۵-dB، پهنای باند وسیع ٤۷ مگاهرتز، بهره قابل توجه ۱۷۸dBi و FTBR 30.7 مشهود است. معیارها برای برجسته کردن ظرفیت آرایه در تضمین سطح برتر از وفاداری سیگنال، شامل طیف گسترده فرکانسی، تقویت سیگنال های دریافتی، و هدایت انتقال به سمت جهت گیری های خاص هستند. این معیارها به صراحت پتانسیل آن را برای برنامه های باند X پیشرفته تایید می کند.